Journal of Magnetism and Magnetic Materials 488 (2019) 165336

Contents lists available at ScienceDirect

Journal of Magnetism and Magnetic Materials

journal homepage: www.elsevier.com/locate/jmmm

Research articles

Ferromagnetism and giant paramagnetism of copper nanoparticles in Cu_m/C nanocomposites

A. Manukyan[a,b], H. Gyulasaryan[a,b], A. Kocharian[c,*], M. Estiphanos[c], O. Bernal[c], E. Sharoyan[b]

[a] Russian-Armenian (Slavonic) University, Armenia
[b] Institute for Physical Research, National Academy of Sciences, Ashtarak 0203, Armenia
[c] California State University, Los Angeles, CA 90032, USA

ARTICLE INFO

Keywords:
Cu@C nanocomposites
Magnetic properties
Size effect
Solid-phase pyrolysis
Solid solutions of phthalocyanines

ABSTRACT

Carbon coated copper nanoparticles, Cu_m/C nanocomposites, were synthesized using solid-phase pyrolysis in solid solutions of copper phthalocyanine and metal free copper phthalocyanine, $(CuPc)_x(H_2Pc)_{1-x}$ where $0 \leqslant x \leqslant 1$. The weight concentration of copper in percentages consistently varies from 0 to 12 wt% and the sizes of copper nanoparticles in samples changes from 2 nm to 500 nm. Samples containing 8 and 12 wt% Cu have a bimodal size distribution. The X-ray diffraction data and HRTEM images show a face-centered cubic structure of Cu nanocrystallites that uniformly distributed in the carbon matrix. The temperature and field dependences of the magnetization in all copper-containing samples exhibit both ferromagnetic and giant-paramagnetic properties in the measured temperature range of 10–300 K. The saturation magnetization of ferromagnetic nanoparticles falls in the range 0.2–1.5 emu/g and weakly depends on the temperature from helium up to the room temperatures. The paramagnetic magnetizations in Cu/C nanocomposites at H = 50 kOe and T = 10 K are practically an order of magnitude higher in all the samples than the ferromagnetic saturation magnetizations. The paramagnetic susceptibilities of the Cu_m/C nanocomposites at 10 K are of the order of $(0.3–1)10^{-4}$ emu/g_{Cu}Oe, which are one and a half to two orders of magnitude higher than the specific paramagnetic susceptibility of the carbon matrix.

1. Introduction

In recent years the evidence of ferromagnetism at the nanoscale level has been intensively studied in metals and/ or other compounds, whose bulk (massive) samples are diamagnetic. These are primarily gold nanoparticles (NPs) – Au, as well as other non-magnetic elements such as Ag, Cu, Pd, and ZnO compounds with functionalized surfaces and linear dimensions within the range of 2–10 nm [1–6]. Due to their unique characteristics these nanomaterials have promising applications for use in optics, spintronics, catalysis, biomedicine, antibacterial therapy, sensing and nanoelectronic devices [7–9].

The magnetic characteristics of nanoparticles depend essentially on the dimensions, as well as on the matrix in which they are implanted. The range of magnetic behavior of these NPs is rather wide: from (enhanced) diamagnetic [10,11] to (super) paramagnetic [12–14] and even ferromagnetic, ranging from helium temperatures to room temperature [1,2]. Several explanations for magnetism in these nanomaterials have been proposed, such as the competing magnetic contributions of the nanoparticle core and its surface [12], the formation of a magnetic moment due to the charge transfer at the nanoparticle-ligand interface [1,2,14,15], induced large orbital angular moment driven by the rotational motion of electrons close to the clusters inner surface [16] and the emergence of self-sustainable (undamped) persistent currents in metallic core [11].

However, until now the origin of this unexpected magnetism has not yet been fully understood. Three important factors can contribute to the magnetic properties of the material in the nanometric scale: quantum-size, surface and ligand effects. As particle sizes decrease, electron transfer without scattering becomes possible i.e. ballistic transport of charge carriers takes place as well as quantum confinement, quantum interference, and tunneling. The fraction of surface atoms with different chemical and structural topologies increases with the decrease of particle sizes and contribution of surface states becomes significant. The interaction with the atoms of the shell (ligand) leads to a charge redistribution followed by a change in physical properties - interface (or ligand) effect. The contribution of surface atoms also significantly enhances the magnetic anisotropy parameter [17], $K_{eff} = K_V + 6\,K_S/D$ where K_V and K_S are the constants of respective volume and surface

* Corresponding author.
E-mail address: armen.kocharian@calstatela.edu (A. Kocharian).

https://doi.org/10.1016/j.jmmm.2019.165336
Received 4 October 2018; Received in revised form 17 February 2019; Accepted 21 May 2019
Available online 22 May 2019
0304-8853/

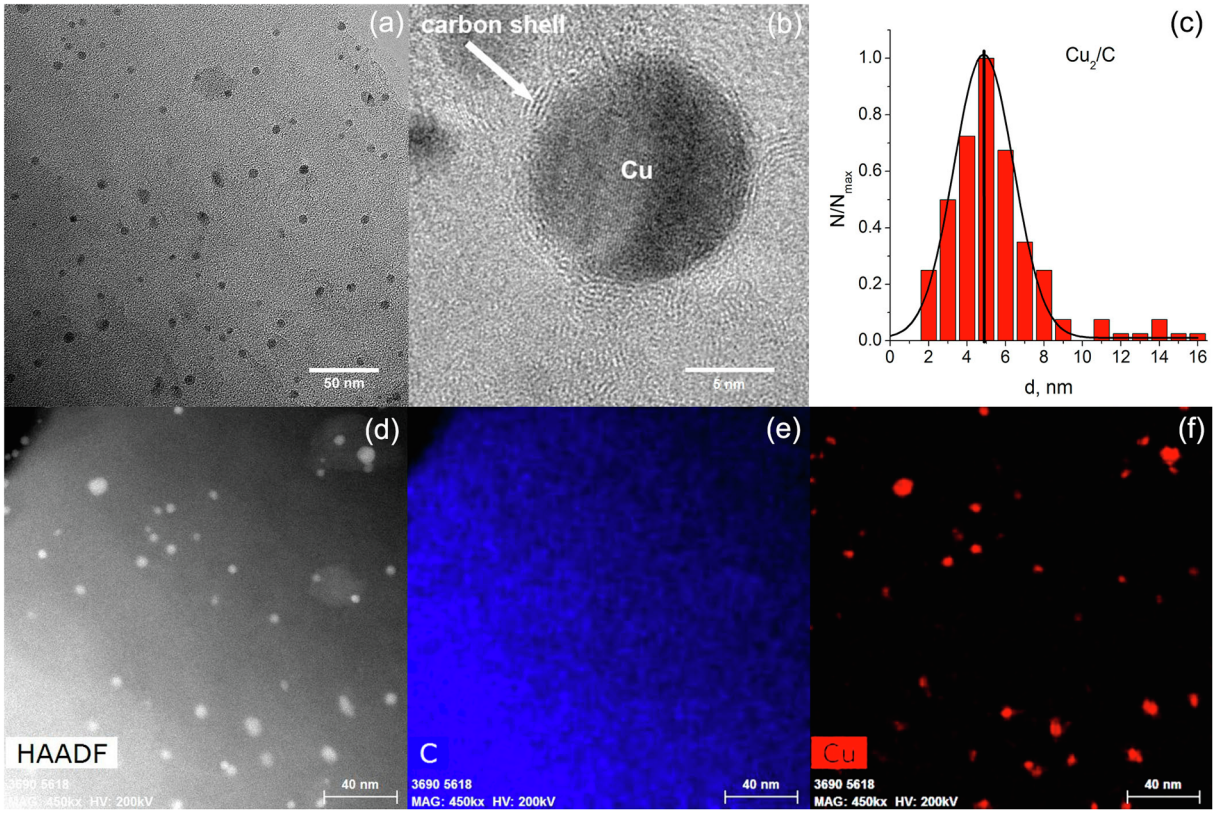

Fig. 1. HRTEM micrographs (a, b) of Cu_2/C sample shows the spherical shape Cu nanoparticles capped by the carbon shell and the corresponding particle size distributions histogram (c). HAADF-STEM image (d) and elemental mapping data for C and Cu (e, f).

magnetic anisotropies. In addition, the exchange, electron-electron interaction and spin-orbit interactions of the electrons are also important factors contributing to magnetism. The ferromagnetic behaviour of copper NPs has previously been investigated [2]. In the case of thiol-capped Cu NPs, ferromagnetism was preserved up to the room temperature, and in the case of amine-capped Cu NPs, a superparamagnetic behavior has been revealed. In this paper we investigate the magnetic properties of Cu NPs in carbon matrix, i.e., Cu/C nanocomposites. Cu NPs encapsulated by graphite-like carbon shell show clear evidence for hysteretic behavior and giant paramagnetism. Here we explore possible approaches to explain the strong magnetism of prepared copper NPs which bulk samples are non magnetic.

2. Experimental

2.1. Samples synthesis

To obtain very fine dispersed copper nanoparticles as well as to study size effects, we first synthesized solid solutions of phthalocyanines: copper phthalocyanine (CuPc, Pc = $C_{32}N_8H_{16}$), and metal free phthalocyanine (H_2Pc). Solid-phase pyrolysis of these solid solutions $(CuPc)_x(H_2Pc)_{1-x}$ where $0 \leqslant x \leqslant 1$ can be represented using the following chemical reaction:

$$[CuPc]_x\,[H_2Pc]_{1-x} \xrightarrow[-8H_2,-4N_2]{T_{pyr},t_{pyr},p} Cu_x + 32C \tag{1}$$

where T_{pyr} is the pyrolysis temperature 850 °C, t_{pyr} is the pyrolysis time 3–15 min and p is the pressure in a reaction ampoule and the value of x is in the interval $0 \leqslant x \leqslant 1$. It is also easy to obtain a relation that relates the concentration of copper in the resulting compounds, expressed in atomic percentages of Cu with the values of x appearing in reaction (1):

$$c_{Cu} = \frac{x}{32 + x} \cdot 100at.\,\% \tag{2}$$

We synthesized a set of stable samples with atomic Cu concentrations equal to 0, 0.5, 1, 2, and 3 at.%. The weight percent corresponding to these samples are 0, 2, 4, 8 and 12 wt% respectively. The studied series of samples are indexed by weight percent Cu_m/C: Cu_0/C, Cu_2/C, Cu_4/C, Cu_8/C and Cu_{12}/C. The values of the copper concentration in the carbon matrix were measured by X-ray fluorescence analysis, which, with an accuracy of 10%, coincide with the calculated values obtained according to formula (2). It is noteworthy to say that X-ray fluorescence analysis and energy dispersive X-ray spectroscopy showed no evidence for the presence of magnetic elements such as Fe, Co, Ni etc. in the measured samples or their concentration must be less than 1 ppm.

2.2. Material characterizations

The elemental composition of the obtained samples was investigated by X-ray Fluorescence Spectrometer Thermo Scientific ARL QUANTAX and Energy dispersive X-ray spectroscopy (EDS) using the Bruker Super-X quad X-ray detectors, combined with high brightness X-FEG (field emission gun). Morphology and sizes of prepared samples were investigated using a FEI Talos F200X field-emission high resolution transmission electron microscopy (HRTEM) and scanning transmission electron microscopy (STEM) at an accelerating voltage of 200 kV. The structure of the nanocomposites was determined using X-ray diffractometer Bruker D2 Phase model # A26X1 (radiation of CuK_α, 1.54060 Å). Magnetic properties of Cu nanoparticles have been studied using vibrating magnetometer (VSM, Quantum Design) in magnetic fields to 50 kOe in a temperature range 10–300 K.

3. Results and discussions

3.1. Structure investigations

The prepared samples are air-stable black powders consisting of a carbon matrix with copper nanocrystallites.

The HRTEM image (Fig. 1a) of Cu/C nanocomposites with Cu concentration of 2 wt% (sample Cu_2/C) clearly shows a uniform distribution of Cu nanoparticles in carbon matrix. The shape of nanoparticles is close to spherical. These nanocomposites have an apparent core-shell structure where Cu nanoparticles coated with graphite-like carbon shells (Fig. 1b) are analogous to the case of Ni/C nanocomposites [18,19]. The carbon shell prevents Cu nanoparticles from further oxidation and aggregation. Fig. 1d,e,f shows the HAADF-STEM image and corresponding elemental data mapping. Using the data of HRTEM and STEM measurements, the corresponding particle size distribution histogram of Cu_2 nanoparticles in Cu_2/C sample is constructed (see Fig. 1c). The solid line represents the fitting curve assuming a Gaussian function. The calculated average diameter (d) of the Cu nanoparticles and the standard deviation (σ) are 5 nm and 1.5 nm respectively. An increase in the concentration of Cu in the carbon matrix leads to an increase in the average diameter of the nanoparticles. In particular, in the case of 4 wt% of Cu (sample Cu_4/C) in carbon matrix, the average diameter of Cu nanoparticles is 10 nm (Fig. 2a). It is interesting to note that in the case of 8 and 12% Cu (samples Cu_8/C and Cu_{12}/C) we have a bimodal size distribution. It should also be noted that small (fine) nanoparticles (2–10 nm) are present in all samples. It is apparent, the mass of these small nanoparticles in Cu_4/C, Cu_8/C and Cu_{12}/C samples is much smaller than in the Cu_2/C sample. In addition, in Cu_8/C and Cu_{12}/C samples, the number of large nanoparticles (average diameters are 300–400 nm) is two orders of magnitude less than that of fine nanoparticles (average sizes of 2–10 nm), while the mass of large nanoparticles is four orders of magnitude more than the mass of small nanoparticles. This is also indicated by the intensity of the peaks of X-ray diffraction spectra.

Fig. 3 represents X-ray diffraction spectra (XRD) of samples with close masses recorded at room temperature, where one can see the peak patterns from Cu and carbon. A broad-scale peak at about 25.5° corresponds to graphite-like carbon structures and other five narrow peaks with angles 2θ = 43.4° (111), 50.5° (200), 74.2° (220), 90° (311) and 95.2° (222) which correspond to copper nanoparticles with a face-centered cubic (fcc) crystalline structure.

3.2. Magnetic measurements

The basic magnetic characteristics Cu_m/C are presented in Figs. 4–7. Magnetic measurements were performed in a wide range of temperatures (10–300 K) and in external magnetic fields up to 50 kOe. Both

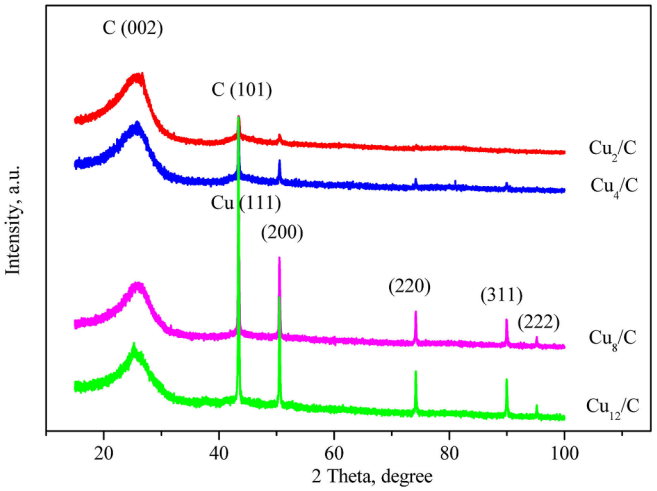

Fig. 3. Room-temperature XRD patterns in Cu_m/C sample series show the peaks of copper and carbon.

structural and magnetic data show that our samples are actually consisting of single-domain ensembles of Cu nanoparticles embedded in a carbon matrix.

The easy axes of magnetization in ferromagnetic nanoparticles are randomly distributed within the sample. Fig. 4 shows the dependence of magnetization on the magnetic field in Cu_m/C series at temperatures of 10 and 300 K, respectively. In the presented curves, diamagnetism of the sample holder is subtracted. The total magnetization of samples, M (H,T), can be presented as a sum of ferromagnetic and paramagnetic contributions: $M(H,T) = M^{FM}(H,T) + \chi_{PM}(T)\,H$. The hysteresis loops measured at the same temperatures are shown on Fig. 5. It should be noted that the ferromagnetic hysteresis loops are somewhat distorted due to the paramagnetic contribution of $\chi_{PM}(T)$ H in the samples, especially at low temperatures.

Analysis of the curves in Fig. 4 lead to the following conclusions: a) the paramagnetic magnetization at T = 10 K is linear function of field up to H = 50 kOe and it is far from saturation; b) paramagnetic magnetizations at H = 50 kOe and T = 10 K practically in all the samples are an order of magnitude higher than the corresponding value of saturation magnetization of ferromagnetic fraction; c) the ratio of the proportions of the paramagnetic fraction to the ferromagnetic fraction, are approximately the same for all samples. Fig. 6 shows the dependence of the paramagnetic susceptibility on the concentration of copper mass (weight percentage), i.e., m (wt%). The paramagnetic susceptibility values of a carbon matrix calculated per gram of the sample in the absence of copper nanoparticles (x = 0, m = 0), and a nickel nanoparticles in Ni_2/C nanocomposites have been added in Fig. 6 for

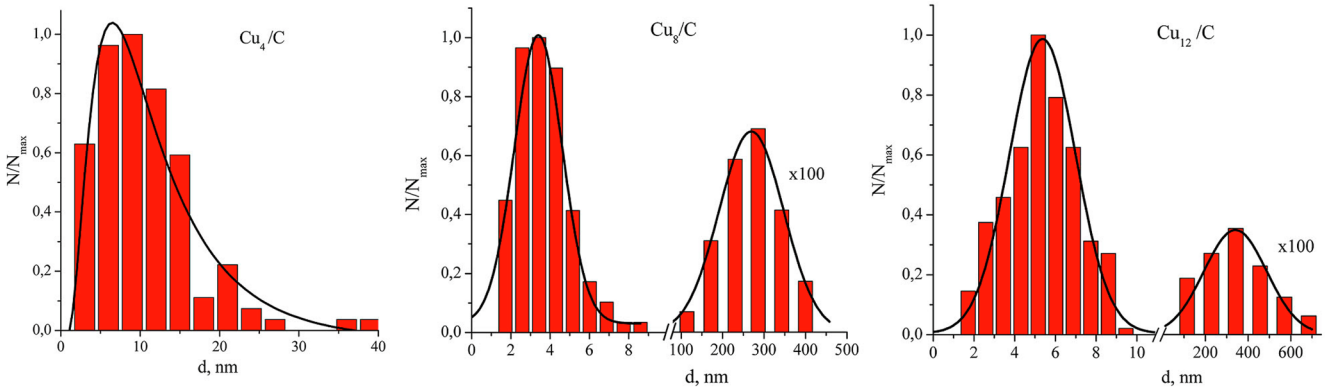

Fig. 2. Size distribution histograms of Cu nanoparticles in Cu_4/C, Cu_8C and Cu_{12}C series. The solid line represents the fitting curve by assuming a lognormal (Cu_4/C) and Gauss function (Cu_8/C, Cu_{12}/C) distributions.

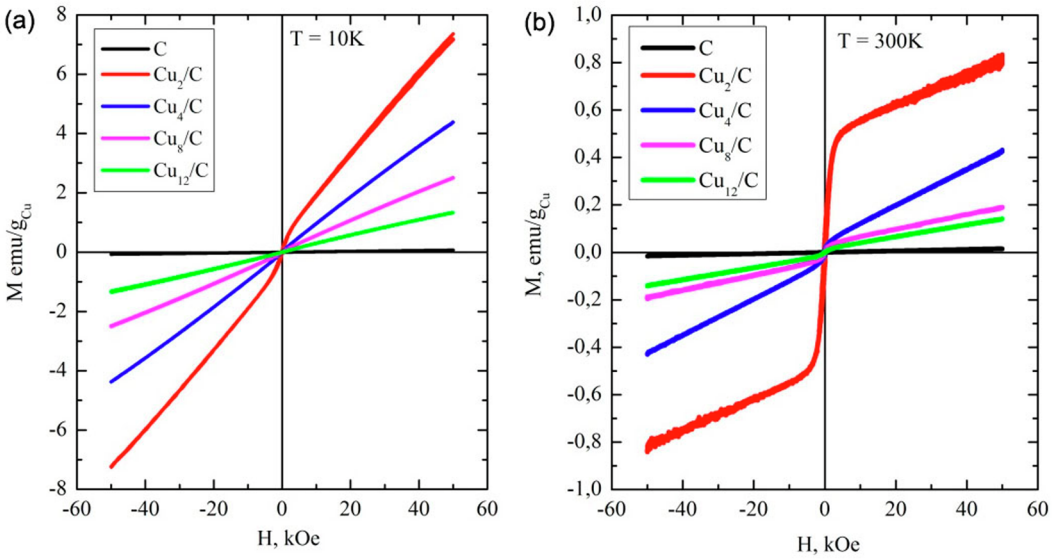

Fig. 4. M versus H in series of Cu_m/C sample series (m = 0, 2, 4, 8 and 12 wt%) at T = 10 K (a) and 300 K (b).

comparison. The increase in the paramagnetic susceptibility by one and a half to two orders is observed in the Cu_m/C samples with respect to the carbon matrix, as well as the surprising similarity of the magnetic properties of the nanocomposites Cu_2/C and Ni_2/C, where the respective average sizes 5 nm and 4 nm of metal nanoparticles are approximately same. The similarity of magnetic properties of Cu_2/C and Ni_2/C is apparently due to the same nature of magnetism in these samples. We assume a giant paramagnetism in Cu_2/C and Ni_2/C samples of quantum-dot dimension is caused by large orbital moments of conduction electrons in ballistic regime [20].

In Fig. 7 the temperature dependences of the magnetization in series of the Cu_m/C samples (m = 0, 2, 4, 8 and 12 wt%) are given, measured in a magnetic field of 50 kOe. Samples in which there is no copper nanoparticles (m = 0, x = 0) correspond to the pyrolysis of the non-metal phthalocyanine. These samples exhibit only paramagnetic properties. The calculated concentration of paramagnetic centers of the carbon matrix is $10^{18} - 10^{19}$ spin/g. The paramagnetism of the carbon matrix is apparently due either to impurity nitrogen atoms or to the electronic states in nanographites at the zig-zag edges. The magnetic properties of the carbon matrix obtained after the solid-phase pyrolysis of a metal free phthalocyanine were also studied in our previous works [21,22]. In series samples with copper - Cu_m/C, at temperatures < 50 K, paramagnetism prevails (see the inset in Fig. 7). At temperatures of 200–300 K, the magnetization varies insignificantly and, obviously, it is mainly due to the ferromagnetic phase of copper nanoparticles in these samples. Estimated values of the saturation magnetization in series of the Cu_m/C samples are 0.2–1.5 emu/g_{Cu}. The maximum value of the saturation magnetization is observed in the sample is Cu_2/C sample with the average d = 5 nm.

What is the nature of ferromagnetism and paramagnetism in the copper NPs? There are a number of factors inherent to metallic nanoparticles, whose massive samples are classical diamagnets. The intrinsic behavior of these nanoparticles within the 2–10 nm range is mainly determined by surface, ligand and quantum-size effects. It is apparent that for d < 10 nm, the fraction of surface atoms sharply increases and, as noted in the introduction, the interaction of metal nanoparticles with the ligand environment becomes substantial. In the earlier studied Ni@C nanocomposites, we observed a sharp drop in magnetization with a decrease in the size of Ni from 40 to 10 nm. The magnetization drop in Ni@C composites results from interaction between Ni nanoparticles and

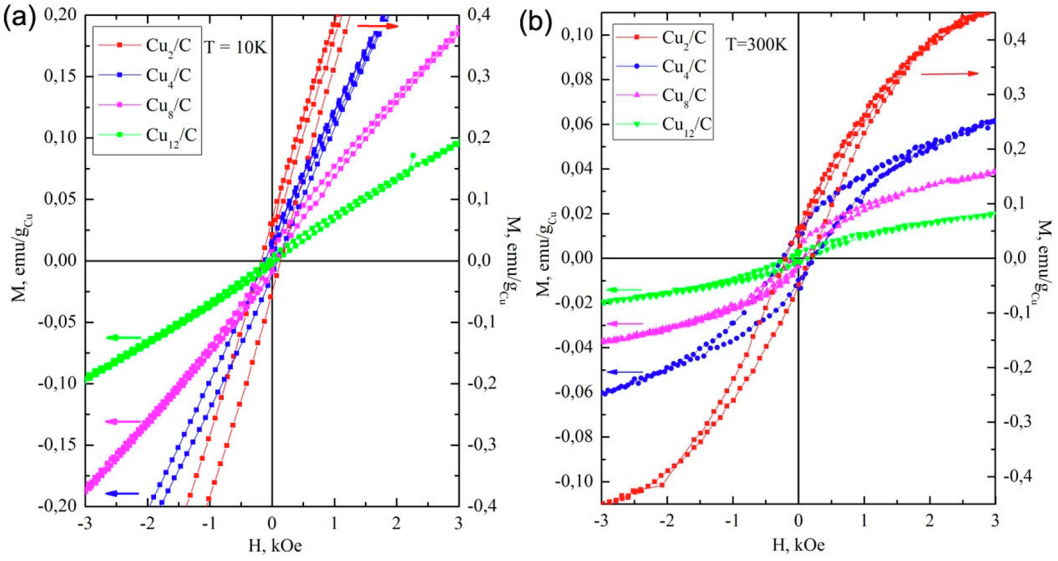

Fig. 5. Hysteresis loops in Cu_m/C sample series (m = 2, 4, 8 and 12 wt%) at T = 10 K (a) and 300 K (b).

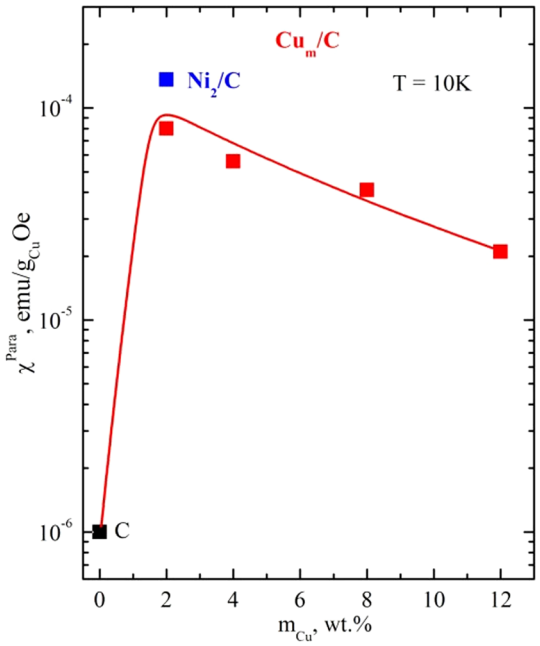

Fig. 6. Dependence of the paramagnetic susceptibility of Cu_m/C nanocomposites on the concentration of copper in weight percentage – m_{Cu} wt% at T = 10 K. Figure also compares the values of the paramagnetic susceptibility of the carbon matrix and Ni_2/C nanocomposites.

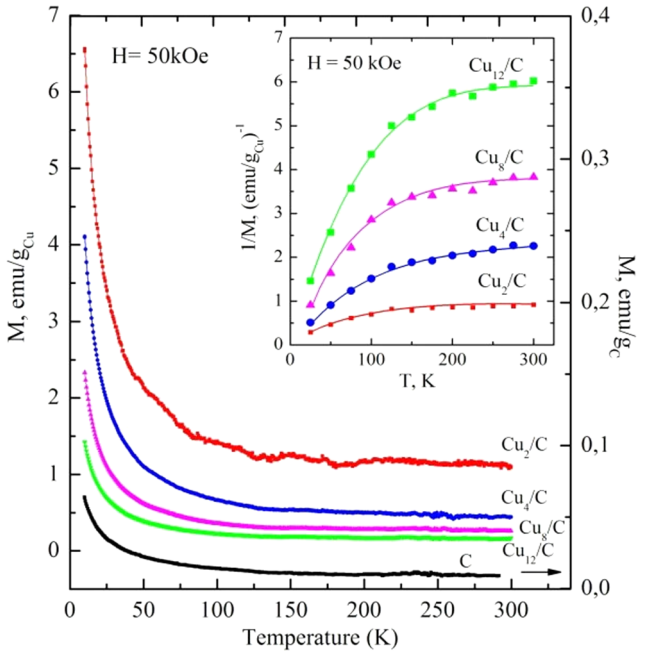

Fig. 7. Magnetization M versus temperature in Cu_m/C sample series (m = 0, 2, 4, 8 and 12 wt%) at H = 50 kOe.

the graphite matrix. Apparently, a significant suppression of Ni local magnetic moment in Ni@C nanocomposites occurs due to the electron transfer from a carbon matrix to nickel. Transfer of electrons on one hand leads to the formation of the "dead" layer consisting of diamagnetic nickel ions described by the following reaction

$$Ni(3d^9 4s^1) + e^- \rightarrow Ni^{1-}(3d^{10}4s^1),$$
$$[FM(Ni) \rightarrow Dia(Ni^{1-})] \quad (3)$$

On the other hand, according to the band model a transfer of electrons on nickel in Ni@C composites leads to reduction of the density of states near the Fermi level.

In the case of Cu_n/C nanocomposites, the values of the work function of electrons from either copper nanoparticles or a curved nanographite structure are not known. We hereby consider two cases of the charge transfers that induce magnetism. The first case is an electron transfer from copper nanoparticles to the curved surface of nanographite matrix. And second case is the reverse transfer. Charge transfers which change the electron configuration of the ground state of Cu can be presented as follows:

$$Cu(3d^{10}4s^1) - e \rightarrow Cu^{1+}(3d^9 4s^1) \quad (4)$$

$$Cu(3d^{10}4s^1) + e \rightarrow Cu^{1-}(3d^{10}4sp) \quad (5)$$

In the first case (Eq. (4)), we have surface and near-surface layers of copper cations with the electron configuration $(3d^9 4s^1)$, which corresponds to the electronic configuration of ferromagnetic nickel. The possibility of occurrence of giant paramagnetism and ferromagnetism in non-magnetic substances with dimensions less than 10 nm were considered in [3,23]. Surface states and their corresponding atomic orbitals with giant magnetic moments have been studied. The second case, i.e. the electron transfer from nano-graphite to copper nanoparticles (Eq. (5)) corresponds to magnetism of delocalized conduction electrons. These electrons form narrow impurity zones causing giant paramagnetism as well as sp-ferromagnetism [24]. Condition for occurrence of ferromagnetism is given by the Stoner criterion, $I_{eff}N(E_F) > 1$, where I_{eff} is the exchange integral and $N(E_F)$ is the density of states near the Fermi energy.

In order to understand the nature of giant paramagnetism and ferromagnetism in M/C nanocomposites, further studies of various diamagnetic metals with narrow size distributions in various ligand (matrix) environments should be analyzed, as well as the application of element-sensitive methods of investigation, along with stationary and resonant magnetic measurements.

4. Conclusions

In the present work, solid solutions $(CuPc)_x(H_2Pc)_{1-x}$ where $0 \leqslant x \leqslant 1$, was synthesized using solid-phase pyrolysis which allowed obtain copper nanoparticles in a carbon matrix. The dilution of copper phthalocyanine with a non-metal phthalocyanine, as well as the variation of the conditions of the solid-phase pyrolysis, provide samples in which the weight concentrations of copper in carbon can be varied from 0 to 12 wt%, and the nanoparticle sizes are from 2 to 500 nm. Our structural studies show that copper nanoparticles form an fcc lattice structure and that they are encapsulated in nano-graphite-like carbon shells. Giant paramagnetism was detected in all Cu_m/C samples, whose paramagnetic susceptibilities are one and a half to two orders of magnitude greater than the paramagnetism observed in the carbon matrix. The paramagnetic susceptibilities in Cu_m/C nanocomposites are of the order of $(0.3 - 1)10^{-4}$ emu/g_{Cu}Oe. In nanocomposite Cu_m/C, the room temperature ferromagnetism is also found, which is apparent due to small copper nanoparticles, the diameters of which are about 2–5 nm. The saturation magnetization of ferromagnetic nanoparticles in the studied samples are in the range 0.2–1.5 emu/g_{Cu} and almost independent on the temperature between the helium and the room temperatures. The maximum value of the saturation magnetization is about 1.5 emu/g_{Cu}, in the Cu_2/C sample with average diameter, $d \approx 5$ nm. The various approaches were also considered arising from a charge transfer from metal to matrix or visa-versa for interpreting our experimental results.

Acknowledgements

This work is dedicated to the memory of our colleague Dr. Armen Mirzakhanyan. This work was supported by a grant from the Russian-Armenian (Slavonic) University and funded by the Russian Federation's

Ministry of Education and Science. The work performed at California State University in Los Angeles was supported by the National Science Foundation-Partnerships for Research and Education in Materials under Grant DMR-1523588.

References

[1] P. Crespo, R. Litran, T.C. Rojas, M. Multigner, J.M. de la Fuente, J.C. Sanchez-Lopez, M.A. García, A. Hernando, S. Penades, A. Fernandez, Permanent magnetism, magnetic anisotropy, and hysteresis of thiol-capped gold nanoparticles, Phys. Rev. Lett. 93 (2004) 087204.
[2] J.S. Garitaonandia, M. Insausti, E. Goikolea, M. Suzuki, J.D. Cashion, N. Kawamura, H. Ohsawa, I. Gil de Muro, K. Suzuki, F. Plazaola, T. Rojo, Revisiting magnetism of capped Au and ZnO nanoparticles: surface band structure and atomic orbital with giant magnetic moment, Nano Lett. 8 (2008) 661–667.
[3] A. Hernando, P. Crespo, M.A. Garca, M. Coey, A. Ayuela, P.M. Echenique, Revisiting magnetism of capped Au and ZnO nanoparticles: surface band structure and atomic orbital with giant magnetic moment, Phys. Status Solidi B 248 (2011) 2352–2360.
[4] S. Trudel, Unexpected magnetism in gold nanostructures: making gold even more attractive, Gold. Bull. 44 (2011) 3–13.
[5] Q.G.L. Nealon, B. Donnio, R. Greget, J.-P. Kappler, E. Terazzi, J.-L. Gallani, Magnetism in gold nanoparticles, Nanoscale 4 (2012) 5244–5258.
[6] T. Shinohara, T. Sato, T. Taniyama, Surface ferromagnetism of Pd fine particles, Phys. Rev. Lett. 91 (2003) 197201.
[7] V.D. Cao, P.P. Nguyen, V.Q. Khuong, C.K. Nguyen, X.C. Nguyen, C.H. Dang, N.Q. Tran, Ultrafine copper nanoparticles exhibiting a powerful antifungal/killing activity against corticium salmonicolor, Bull. Korean Chem. Soc. 35 (2014) 2645–2648.
[8] L. Shi, R.-P. Liang, J.-D. Qiu, Controllable deposition of platinum nanoparticles on polyaniline-functionalized carbon nanotubes, J. Mater. Chem. 22 (2012) 17196–17203.
[9] N. Griffete, H. Frederich, A. Maitre, S. Ravaine, M.M. Chehimi, C. Mangeney, Inverse opals of molecularly imprinted hydrogels for the detection of bisphenol A and pH sensing, Langmuir 28 (2012) 1005–1012.
[10] E. Guerrero, M.A. Munoz Marquez, M.A. García, P. Crespo, E. Fernandez Pinel, A. Hernando, A. Fernandez, Surface plasmon resonance and magnetism of thiol-capped gold nanoparticles, Nanotechnology 19 (2008) 175701.
[11] R. Greget, G.L. Nealon, B. Vileno, P. Turek, C. Meny, F. Ott, A. Derory, E. Voirin, E. Riviere, A. Rogalev, Magnetic properties of gold nanoparticles: a room-temperature quantum effect, Chem. Phys. Chem. 13 (2012) 3092–3097.
[12] Y. Yamamoto, T. Miura, M. Suzuki, N. Kawamura, H. Miyagawa, T. Nakamura, K. Kobayashi, T. Teranishi, H. Hori, Direct observation of ferromagnetic spin polarization in gold nanoparticles, Phys. Rev. Lett. 93 (2004) 116801.
[13] Y. Negishi, H. Tsunoyama, M. Suzuki, N. Kawamura, M.M. Matsushita, K. Maruyama, T. Sugawara, T. Yokoyama, T. Tsukuda, X-ray magnetic circular dichroism of size-selected, thiolated gold clusters, J. Am. Chem. Soc. 128 (2006) 12034–12035.
[14] J. Bartolome, F. Bartolome, L.M. García, A.I. Figueroa, A. Repolles, M.J. Martínez, F. Luis, C. Magen, S. Selenska-Pobell, F. Pobell, T. Reitz, R. Schonemann, T. Herrmannsdorfer, M. Merroun, A. Geissler, F. Wilhelm, A. Rogalev, Strong paramagnetism of gold nanoparticles deposited on a Sulfolobus acidocaldarius S layer, Phys. Rev. Lett. 109 (2012) 247203.
[15] M. Suda, N. Kameyama, M. Suzuki, N. Kawamura, Y. Einaga, Reversible photo-tuning of ferromagnetism at Au-S interfaces at room temperature, Angew. Chem. 47 (2008) 160–163.
[16] H.-B. Li, W. Wang, X. Xie, Y. Cheng, Z. Zhang, H. Dong, R. Zheng, W.-H. Wang, F. Lu, H. Liu, Electronic structure and ferromagnetism modulation in Cu/Cu_2O interface: impact of interfacial Cu vacancy and its diffusion, Sci. Rep. 5 (2015) 15191.
[17] F. Bodker, S. Morup, S. Linderoth, Surface effects in metallic iron nanoparticles, Phys. Rev. Lett. 72 (1994) 282.
[18] A.S. Manukyan, A.A. Mirzakhanyan, G.R. Badalyan, G.H. Shirinyan, A.G. Fedorenko, N.V. Lianguzov, Yu.I. Yuzyuk, L.A. Bugaev, E.G. Sharoyan, Nickel nanoparticles in carbon structures prepared by solid-phase pyrolysis of nickel-phthalocyanine, J. Nanopart. Res. 14 (2012) 982-1-7.
[19] A.S. Manukyan, A.A. Mirzakhanyan, L. Sajti, R.D. Khachaturyan, E. Kaniukov, L. Lobanovsky, E. Sharoyan, Magnetic properties of carbon-coated Ni nanoparticles prepared by solid-phase pyrolysis of nickel-phthalocyanine, Nano 10 (2015) 1550089-1.
[20] A. Manukyan, A. Elsukova, A. Mirzakhanyan, H. Gyulasaryan, A. Kocharian, S. Sulyanov, M. Spasova, F. Roumer, M. Farle, E. Sharoyan, Structure and size dependence of the magnetic properties of Ni@C nanocomposites, J. Magn. Magn. Mater. 467 (2018) 150–159.
[21] A.S. Manukyan, A.A. Mirzakhanyan, R.D. Khachaturyan, A.T. Gyulasaryan, A.N. Kocharian, Yu.I. Yuzyuk, E.G. Sharoyan, Structure and magnetic properties of carbon microspheres prepared by solid-phase pyrolysis of organic compounds, J. Contemp. Phys. (Armenian Ac. Sci.) 50 (2015) 195–199.
[22] E. Sharoyan, A. Mirzakhanyan, H. Gyulasaryan, C. Sanchez, A. Kocharian, O. Bernal, A. Manukyan, Ferromagnetism of nanographite structures in carbon microspheres, IEEE Trans. Magn. 52 (2016) 1–3.
[23] A. Hernando, M.A. Garcia, Magnetism induced by capping of non-magnetic ZnO nanoparticles, J. Nanopart. Res. 13 (2011) 5595–5602.
[24] D.M. Edwards, M.I. Katsnelson, High-temperature ferromagnetism of sp electrons in narrow impurity bands: application to CaB_6, J. Phys.: Condens. Matter 18 (2006) 7209–7225.